Journal of Power Sources 196 (2011) 9786–9791

Contents lists available at ScienceDirect

Journal of Power Sources

journal homepage: www.elsevier.com/locate/jpowsour

$NH_4V_3O_8$/carbon nanotubes composite cathode material with high capacity and good rate capability

Haiyan Wang[a,*], Kelong Huang[a,*], Yu Ren[b], Xiaobing Huang[c], Suqin Liu[a], Wenjie Wang[a]

[a] School of Chemistry and Chemical Engineering, Central South University, Changsha, 410083, PR China
[b] School of Chemistry, University of St Andrews, Fife KY16 9ST, UK
[c] College of Chemistry and Chemical Engineering, Hunan University of Arts and Science, Changde 415000, PR China

ARTICLE INFO

Article history:
Received 21 March 2011
Received in revised form 5 July 2011
Accepted 4 August 2011
Available online 10 August 2011

Keywords:
Li-ion battery
Ammonium trivanadate
Carbon nanotubes
Hydrothermal method
Cycling stability

ABSTRACT

$NH_4V_3O_8$/carbon nanotubes (CNTs) composites are synthesized by one-step hydrothermal method. All the samples show the flake-like morphology with the width of up to 5 μm and thickness of 500 nm and the CNTs are clearly observed on the surface of modified $NH_4V_3O_8$. It is found that incorporation of 0.5 wt% CNTs into $NH_4V_3O_8$ could greatly improve its discharge capacity and cycling stability. It delivers a maximum discharge capacity of 358.7 mAh g^{-1} at 30 mA g^{-1}, 55 mAh g^{-1} larger than that of the pristine one. At 150 mA g^{-1}, the composite shows 226.2 mAh g^{-1} discharge capacity with excellent capacity retention of 97% after 100 cycles. The much improved electrochemical performance of $NH_4V_3O_8$ is attributed to incorporation of CNTs, which facilitates the interface charge transfer and Li^+ diffusion.

1. Introduction

Vanadium oxides and their derivatives have attracted a lot of attention as cathode material for Li-ion battery due to their easy synthesis, low cost and high capacity [1–6]. Of these the most studied is lithium trivanadate (LiV_3O_8), which possesses good structural stability. LiV_3O_8 is composed of two basic structure units (VO_6 octahedron and VO_5 distorted trigonal bipyramid) and the $V_3O_8^-$ layers are held together through the interaction with the interlayered lithium ions [4]. Preparation methods strongly influence its electrochemical properties [5,6]. To the best of our knowledge, LiV_3O_8 could not be synthesized by one-step hydrothermal method. In our previous work, we employed one-step hydrothermal approach to obtain flake-like $NH_4V_3O_8$, which exhibited a maximum discharge capacity of 225.9 mAh g^{-1} with good cycling stability [7]. Recently, we find that $NH_4V_3O_8$ flakes with discharge capacity up to 310 mAh g^{-1} could be achieved via surfactant-free hydrothermal method. However, the thickness of flakes is very large, which would influence the rapid transferring of Li^+ and e^-, leading to an inferior rate capability. Therefore, much work should be done for its application in Li-ion battery.

Carbon nanotubes (CNTs) are well known for excellent electronic conductivity and mechanical property. And CNTs-modified Li_2FeSiO_4 [8] has been prepared, which demonstrates much improved rate performance. There is no doubt that incorporation of CNTs into $NH_4V_3O_8$ flakes would be beneficial to the electronic conductivity. More importantly, CNTs attached to $NH_4V_3O_8$ flake could probably form an interesting network to bridge the separated flakes. Accordingly, in current work, modified $NH_4V_3O_8$ with CNTs are synthesized. As expected, $NH_4V_3O_8$/0.5 wt% CNTs composite has much higher discharge capacity, coupled with better rate capability and cycling stability. There is no observable capacity loss after 100 cycles at 150 mA g^{-1}.

2. Experimental

2.1. Synthesis and characterization

Firstly, 1.755 g of NH_4VO_3 was dissolved in distilled water under gentle temperature with vigorous stirring. 7.5 or 37.5 mg of CNTs (corresponding to mass fraction of 0.5% and 2.5% to final theoretical $NH_4V_3O_8$, respectively) was dispersed for 1 h under ultrasonic bath using polyvinyl pyrrolidone as dispersant and then added into NH_4VO_3 solution. CNTs were provided by Chengdu Organic Chemicals Co. Ltd and pre-treated according to Ref. [9]. As follow, a proper amount of hydrochloric acid was added to adjust the pH value to ca. 3.5. The mixed solution (~40 ml) was then transferred into a 50 ml Teflon lined stainless steel autoclave. The autoclave was heated

* Corresponding author. Tel.: +86 731 88879850; fax: +86 731 88879850.
E-mail addresses: wanghy419@126.com (H. Wang), klhuang@mail.csu.edu.cn (K. Huang).

0378-7753/$ – see front matter © 2011 Elsevier B.V. All rights reserved.
doi:10.1016/j.jpowsour.2011.08.015

at 180 °C for 48 h and then cooled to room temperature naturally. The precipitate was filtered, washed with distilled water for three times and then dried at 80 °C overnight. For comparison, pristine $NH_4V_3O_8$ was also prepared by the same procedure without CNTs.

All X-ray diffraction (XRD) data were given by a Philips X-Pert system (Cu-Kα radiation) with a step of 0.02°. Fourier transform infrared (FT-IR) spectra were recorded using Nicolet 6700 FT-IR spectrometer. Morphological studies were conducted using a JSM6430F scanning electron microscopy (SEM). Different scanning calorimetry and thermal gravimetry (DSC/TG) for sample without SDBS was carried out with a NETZSCH STA 449 C differential scanning calorimeter under N_2 atmosphere at a ramping rate of 10 °C min^{-1}. The contents of CNTs in the composites are 0.55 wt%, 2.41 wt%, respectively, characterized by Vario ELIII CHN elemental analysis, approaching to 0.5 wt% and 2.5 wt%.

2.2. Electrochemical measurements

The electrochemical cells were constructed by mixing the active material, polyvinylidene fluoride (PVDF), and Super S carbon in the weight ratio of 80:10:10. Tetrahydrofuran was used as solvent. The slurry was cast onto Al foil using a Doctor-Blade technique. After solvent evaporation at room temperature and heating at 80 °C under vacuum for 8 h, the electrodes were cut into disks and assembled into CR2016 coin-type cells with commercial electrolyte (Merck; 1 M $LiPF_6$ in 1:1 v/v ethylene carbonate/dimethyl carbonate) and a Li metal as counter electrode. The cells were cycled between 1.5 and 4.0 V (versus Li/Li^+) with a Land CT2001A system. Cyclic voltammetry (CV) was operated using electrochemical station (Shanghai Chenhua, China) with scan rate 0.1 mV s^{-1}. Electrochemical impedance spectroscopy (EIS) was recorded by Solartron analytical instrument over the frequency range from 500 kHz to 10 mHz with an amplitude of 5 mV. Before testing, the cell was cycled for three CV and then kept at 2.9 V for 8 h.

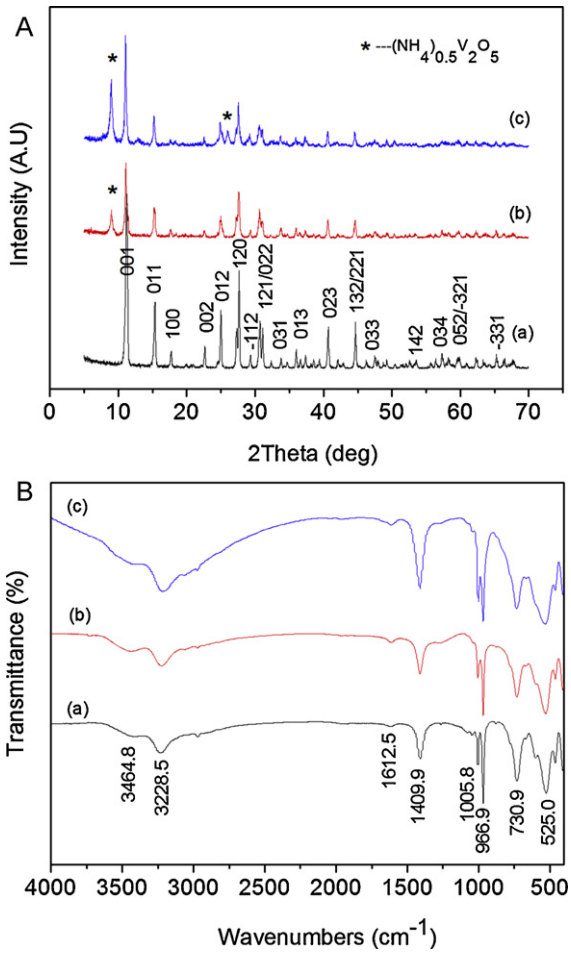

Fig. 1. XRD patterns (A) and FT-IR spectra (B) of as-prepared samples: (a) $NH_4V_3O_8$, (b) $NH_4V_3O_8$/0.5 wt% CNTs, (c) $NH_4V_3O_8$/2.5 wt% CNTs.

3. Results and discussion

Fig. 1(A) shows XRD patterns of as-prepared materials. All diffraction peaks of pattern (a) could be indexed into a pure $NH_4V_3O_8$ phase with monoclinic structure and $P2_1/m$ space group (JCPDS card No. 88-1473). The lattice parameters are a = 0.5011 nm, b = 0.8458 nm, c = 0.7948 nm and β = 96.66°, which are slightly different from the literature values [7,10]. The pattern b and c both indicate the diffraction peaks due to $NH_4V_3O_8$. However, additional peak at about 2θ = 8.9° is observed in pattern b and c. It is worthwhile to note that the intensity of this peak increases with increasing of CNTs content, indicating that more secondary phase appears in the final product. As known, the structure of vanadate oxide is strongly dependent on the experimental conditions, such as pH value, addition agents, etc. [2]. $(NH_4)_{0.5}V_2O_5$ in our previous report [11] has the prominent diffraction peak at 2θ = 8.9°. The reduction of surface $NH_4V_3O_8$ by the attached CNTs may take place during high temperature hydrothermal process. It is deduced thereby that appearance of diffraction peak at 2θ = 8.9° is probably attributed to $(NH_4)_{0.5}V_2O_5$ on the surface of $NH_4V_3O_8$. The hypothesis is further confirmed by the following CV results. The more amount of CNTs, more $(NH_4)_{0.5}V_2O_5$ phase in the product. All three samples show the similar FT-IR curves (Fig. 1(B)), with absorption bands at ca. 3464.8, 3228.5, 1612.5, 1409.9, 1005.8, 966.9, 730.9 and 525.0 cm^{-1}. Bands at 1005.8 and 966.9 cm^{-1} are due to V=O stretching of distorted octahedral and distorted squarepyramids, while those at 730.9 and 525.0 cm^{-1} are assigned to asymmetric and symmetric stretching vibration of V–O–V bonds [12]. Meanwhile, bands at 3235.9 and 1410.5 cm^{-1} are attributed to asymmetric stretching vibrations and symmetric bending vibration of NH_4^+ [13]. Crystal water is verified by two weak bands at 3464.8 and 1612.5 cm^{-1} [7]. Therefore, the as-prepared materials with and without CNTs could be written as $NH_4V_3O_8{\cdot}xH_2O$.

DSC/TG tests for $NH_4V_3O_8$ and $NH_4V_3O_8$/0.5 wt% CNTs were carried out to determine the amount of crystal water in each formula unit. As shown in Fig. 2, both samples indicate an obvious exothermal peak between 220 and 450 °C in DSC curve with the similar mass loss, which corresponds to the decomposition of ammonium trivanadate in Eq. (1).

$$2NH_4V_3O_8 \cdot xH_2O \xrightarrow{\Delta} 3V_2O_5 + 2NH_3\uparrow + (1+2x)H_2O\uparrow \quad (1)$$

In the case of the slight mass loss after 450 °C for CNTs modified sample, it is attributed to the reduction of CNTs. According to the Eq. (1) and the mass loss value, the crystal water in $NH_4V_3O_8{\cdot}xH_2O$ without CNTs is estimated as 0.40, while that for $NH_4V_3O_8$/0.5 wt% CNTs is about 0.37. Considering the similar value of the crystal water, its effect on the electrochemical performance for $NH_4V_3O_8$ and $NH_4V_3O_8$/0.5 wt% CNTs could be almost the same.

As shown in Fig. 3a–c, all three samples have flake-like morphology. The width of flakes is up to 5 μm and the thickness is about 500 nm. A smooth and clean surface is observed for bare sample (Fig. 3a). For CNTs-modified $NH_4V_3O_8$, CNTs are easily observed on the surface of $NH_4V_3O_8$, some of which are integrated into bulk material. When the amount of CNTs was increased to 2.5 wt%, uneven surface and more CNTs could be observed (Fig. 3c). CV comparison (Fig. 4a–c) indicates much difference. The pristine $NH_4V_3O_8$ shows two pairs of redox peaks, with oxidation peaks at 1.84, 3.02 V and corresponding reduction peaks at 1.72, 2.89 V, respectively. A

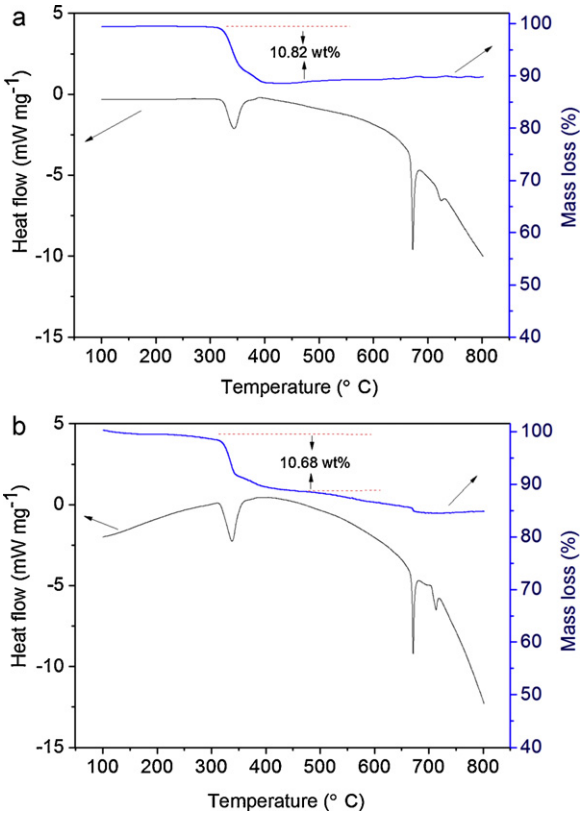

Fig. 2. DSC/TG curves of as-prepared samples: (a) $NH_4V_3O_8$, (b) $NH_4V_3O_8$/0.5 wt% CNTs.

slight pair of redox peak at 2.62 and 2.45 V is also observed. Note that appearance of a new pair of redox peak at 3.72 and 3.66 V and increasing intensity of redox peak at 2.62 and 2.50 V when CNTs adding imply that structure of $NH_4V_3O_8$ has changed a little, which is consistent with XRD results. The redox peak at 2.62 and 2.50 V becomes the prominent one for $NH_4V_3O_8$/2.5 wt% CNTs, which is in accordance with that of $(NH_4)_{0.5}V_2O_5$ [11]. It further confirms that too much CNTs would result in the reduction of V^{5+} to form $(NH_4)_{0.5}V_2O_5$.

Cycling performance and the 30th load curve (inset) of $NH_4V_3O_8$ with different contents of CNTs at 30 mA g^{-1} are shown in Fig. 5. The pristine sample delivers a gradual increasing discharge capacity from 229.1 to 303.8 mAh g^{-1} in the first 5 cycles. A slight capacity fading is observed in the following 10 cycles. After that, more stable capacity is maintained, with 258.5 mAh g^{-1} after 30 cycles. It shows improved electrochemical performance than that in Ref. [7] probably due to the inferior crystallinity from the XRD results. As we know, the higher the relative intensity of diffraction peak (0 0 1) for MV_3O_8 (M = Li^+, NH_4^+), the better the degree of crystallinity. Unfortunately, the preferential ordering of crystal is disadvantageous to the Li^+ intercalation and de-intercalation since it would lead to a long Li^+ diffusion path [7,14]. $NH_4V_3O_8$/0.5 wt% CNTs also shows the similar tendency. However, the composite exhibits much better electrochemical performance with a maximum discharge capacity of 358.7 mAh g^{-1}, 55 mAh g^{-1} higher than that of the pristine one and 309.9 mAh g^{-1} remaining after 30 cycles. As for $NH_4V_3O_8$/2.5 wt% CNTs, it shows severe capacity fading even though its initial discharge capacity is greatly increased to 366.7 mAh g^{-1}. The improved discharge capacity should be due to incorporation of CNTs, which not only greatly improves the surface electronic conductivity of $NH_4V_3O_8$, but also acts as conductive bridges for thick flakes. Structural change is involved in term of poorer cycling stability when adding too much CNTs, which

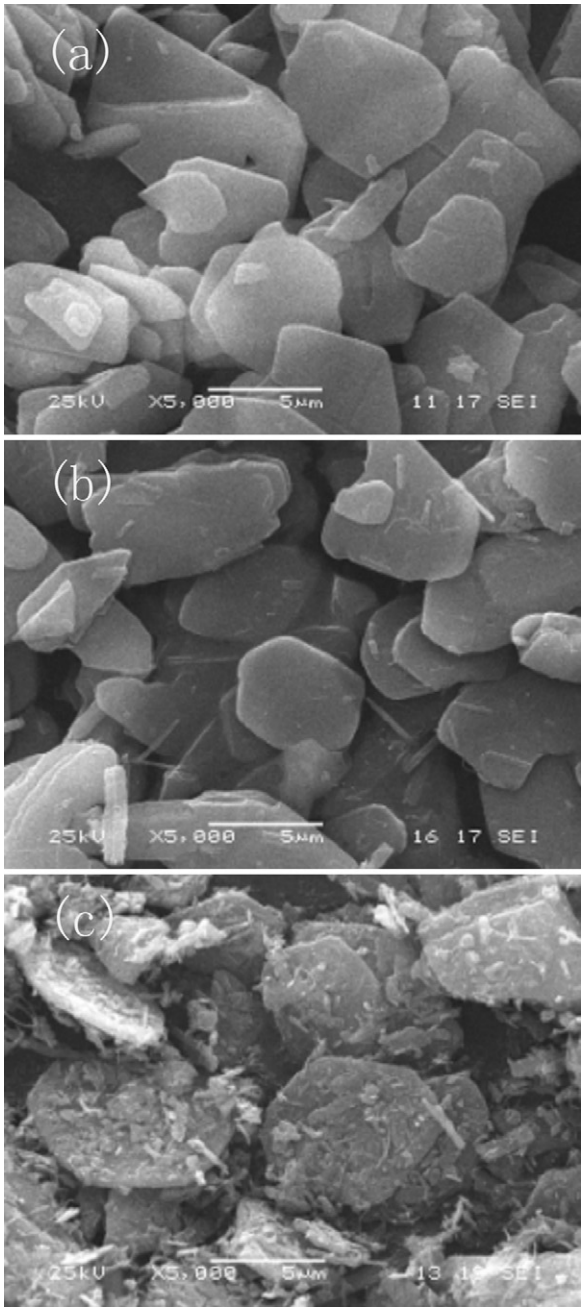

Fig. 3. SEM images of $NH_4V_3O_8$ (a), $NH_4V_3O_8$/0.5 wt% CNTs (b), and $NH_4V_3O_8$/2.5 wt% CNTs (c).

is verified by XRD and CV results. Based on our previous work, $(NH_4)_{0.5}V_2O_5$ possesses inferior cycling stability in comparison with $NH_4V_3O_8$ [11]. However, it is interesting to note that $NH_4V_3O_8$ with a slight amount of CNTs not only shows good cycling stability but also enhanced discharge capacity. The related explanation is proposed in the following paragraph. The Much better plateaus retention ability for $NH_4V_3O_8$/0.5 wt% CNTs is also seen in inset load curves in Fig. 5.

Rate performance of $NH_4V_3O_8$, $NH_4V_3O_8$/0.5 wt% CNTs and $NH_4V_3O_8$/2.5 wt% CNTs was compared at various current densities from 15 to 300 mA g^{-1} (Fig. 6). Fig. 6(b) records the charge–discharge curves of $NH_4V_3O_8$/0.5 wt% CNTs at different rates. The discharge capacity of $NH_4V_3O_8$ at 15, 90, 180 and 300 mA g^{-1} is 309.3, 209.8, 168.8 and 141.2 mAh g^{-1}, respectively. While that of $NH_4V_3O_8$/0.5 wt% CNTs increases to 358.0,

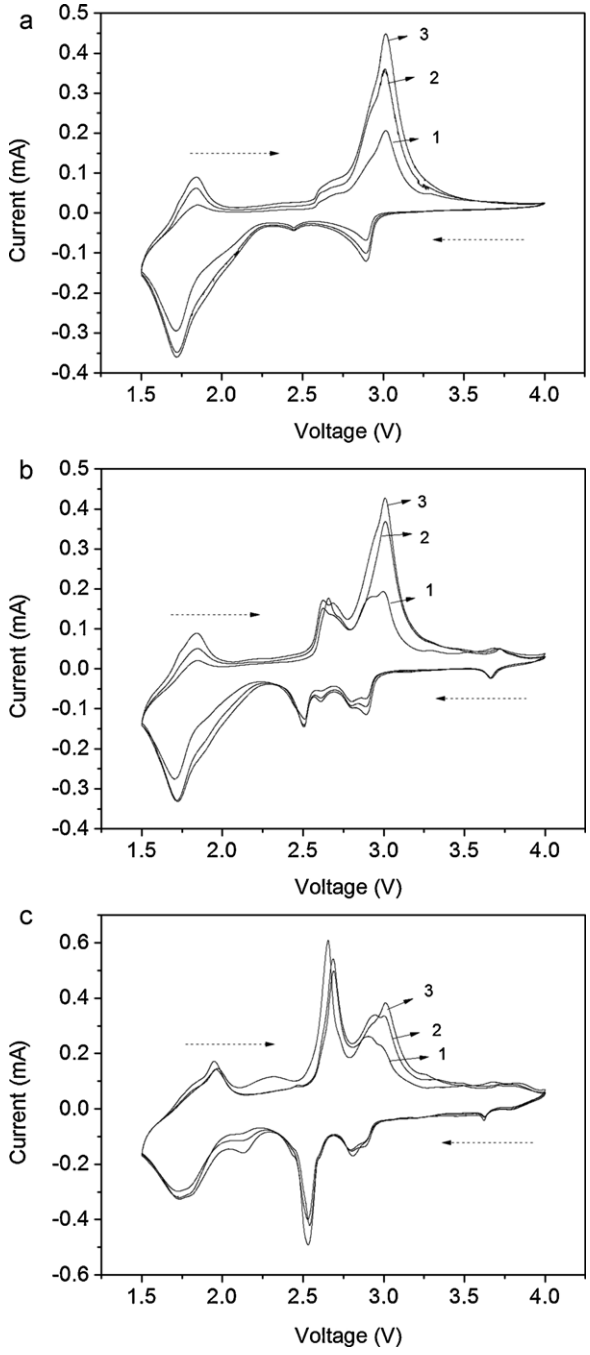

Fig. 4. CV curves of $NH_4V_3O_8$ (a), $NH_4V_3O_8$/0.5 wt% CNTs (b), and $NH_4V_3O_8$/2.5 wt% CNTs (c).

255.8, 213.4 and 190.3 mAh g^{-1}, respectively. Surprisingly, no obvious capacity fading is observed for both samples at relatively high current density. With regard to $NH_4V_3O_8$/2.5 wt% CNTs, the corresponding discharge capacity is 356.9, 256.9, 219.4 and 183.9 mAh g^{-1}, respectively. The cycling performance is much poorer in comparison with the $NH_4V_3O_8$ and $NH_4V_3O_8$/0.5 wt% CNTs. It should be noted that discharge capacity of the pristine one decreases a lot with the increasing of current density, implying poor electronic conductivity, which is partially attributed to the large thickness of flakes. It also should be pointed out that all three samples show poorer cycling stability at a low current density (15 mA g^{-1}), which is probably attributed to capacity loss between 1.5 and 2.0 V. Fig. 6(b) suggests that more Li sites between

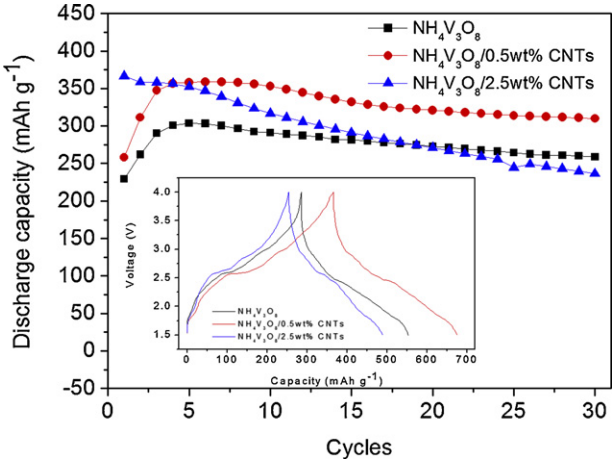

Fig. 5. Cycling performance and the 30th load curves (inset) of $NH_4V_3O_8$, $NH_4V_3O_8$/0.5 wt% CNTs and $NH_4V_3O_8$/2.5 wt% CNTs between 1.5 and 4.0 V at 30 mA g^{-1}.

1.5 and 2.0 V could be used at lower current density, however, such Li sites possess inferior Li^+ insertion/extraction reversible ability. Long cycling test at 150 mA g^{-1} is also shown (Fig. 7). All three cells were first cycled three times at 30 mA g^{-1} to activate the electrodes. The activation is necessary based on the increased discharge capacity in Fig. 6(a). The pristine electrode presents a discharge capacity of 181.5 mAh g^{-1} and capacity retention of 95.2% after 100 cycles. It is much better than that (81.9%) of $(NH_4)_{0.5}V_2O_5$ [11]. The result agrees well with poorer cycling stability of $NH_4V_3O_8$/2.5 wt% CNTs due to appearance of more $(NH_4)_{0.5}V_2O_5$ phase. Accordingly, dis-

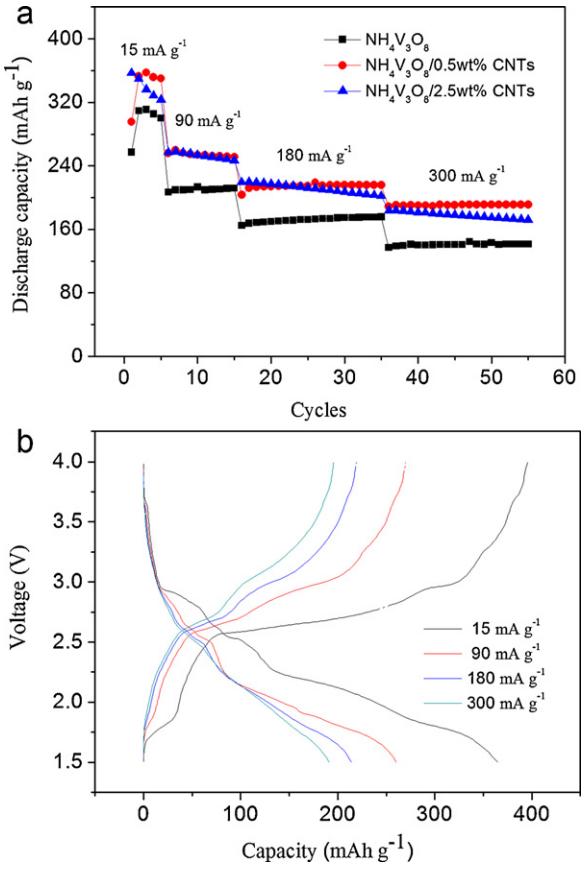

Fig. 6. Rate capability of $NH_4V_3O_8$, $NH_4V_3O_8$/0.5 wt% CNTs and $NH_4V_3O_8$/2.5 wt% CNTs between 1.5 and 4.0 V.

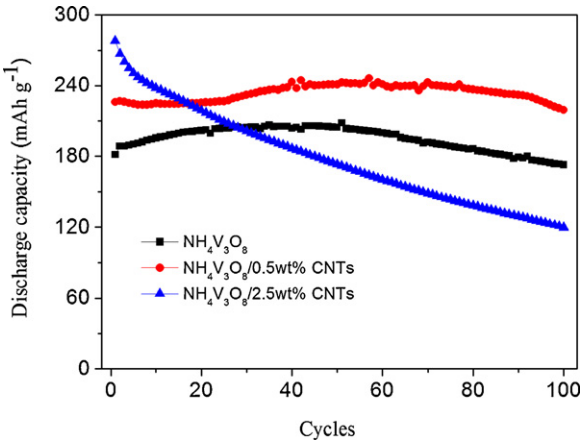

Fig. 7. Long cycling performance of $NH_4V_3O_8$, $NH_4V_3O_8$/0.5 wt% CNTs and $NH_4V_3O_8$/2.5 wt% CNTs between 1.5 and 4.0 V at 150 mA g^{-1}.

charge capacity of $NH_4V_3O_8$/0.5 wt% CNTs is 226.2 mAh g^{-1} and capacity retention is about 97%. 2.5 wt% CNTs coated sample shows an initial discharge capacity of 278.0 mAh g^{-1} and poor cycling stability, only 120.0 mAh g^{-1} retaining after 100 cycles. It reveals that adding too much CNTs would harm the cycling performance of the sample. As shown in Fig. 1, there are a few $(NH_4)_{0.5}V_2O_5$ in the $NH_4V_3O_8$/0.5 wt% CNTs. Conventionally, the cycling stability should be affected to some extent. Why its cycling stability is even better than that pristine one? The probable reasons are proposed as follows: (1) the pristine $NH_4V_3O_8$ possesses the poor ion conductivity, confirmed by the EIS results in Fig. 8, which would affect the material's cycling stability; (2) 0.5 wt% CNTs is a suitable coating amount for $NH_4V_3O_8$, which greatly benefits the ion and electrical conductivity but without the much expense of cycling life because of the small amount. It is possible that the effect of the resulted $(NH_4)_{0.5}V_2O_5$ impurity on the cycling stability is much less than that due to the increased conductivity and interface chemistry; (3) the amount of $(NH_4)_{0.5}V_2O_5$ on the surface of $NH_4V_3O_8$ should be very small and it could be considered as a very thin and uniform coated layer, which would ameliorate the interface chemistry and probably play an important role in stabilizing the structure when cycling at high rate. Nevertheless, $NH_4V_3O_8$/0.5 wt% CNTs here shows excellent cycling stability and good rate capability. To the best of our knowledge, $NH_4V_3O_8$ composite here indicates the comparable electrochemical performance (not only discharge capacity, but also cycling stability at relatively high current densities) with LiV_3O_8 nanorod as reported by Zhou and co-workers [6], which is considered as one of the best LiV_3O_8 in terms of electrochemical properties.

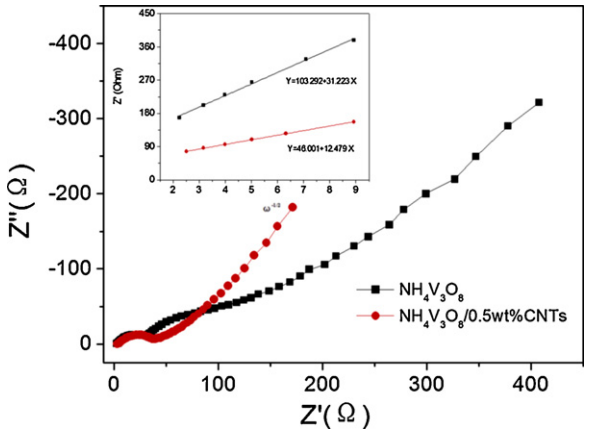

Fig. 8. Nyquist plots and the inset relationship curve between Z' and $\omega^{-1/2}$ in the low frequency of $NH_4V_3O_8$ and $NH_4V_3O_8$/0.5 wt% CNTs at 2.9 V after 3 CV.

Fig. 8 depicts the Nyquist plots and the inset relationship curve between Z' and $\omega^{-1/2}$ in the low frequency of $NH_4V_3O_8$ and $NH_4V_3O_8$/0.5 wt% CNTs at 2.9 V after 3 CV. As can be seen, $NH_4V_3O_8$ shows two depressed semicircles in the high-mediate frequency region and a straight line in the low-frequency region. The high frequency semicircle should be due to the interface parameters such as porous nature of electrode, surface film contribution, and/or the bulk of material while the slop line is due to diffusion of Li^+ into solid state electrodes (Warburg impedance) [15–17]. The diameter value of mediate semicircle on Z_{real} axis is approximately equal to charge transfer resistance (R_{ct}). However, $NH_4V_3O_8$/0.5 wt% CNTs only exhibits a visible semicircle in high-mediate frequency region. In our opinion, incorporation of CNTs could greatly reduce charge transfer resistance so that the two semicircles in the high-mediate frequency region could not separate well. In fact, the separated two semicircles can be observed after 100 cycles. Therefore, as seen, there is a remarkable decrease in R_{ct} after incorporation of CNTs. Li^+ diffusion coefficient could be calculated from the low frequency plots according to the following Eqs. (2) and (3) [18,19]:

$$D = \frac{R^2T^2}{2A^2n^4F^4C^2\sigma^2} \quad (2)$$

where R is the gas constant, T is the absolute temperature, A is the surface area, n is the number of electrons per molecule during oxidation, F is the Faraday constant, C is the concentration of Li^+, σ is the Warburg factor which is relative with Z':

$$Z' = R_D + R_L + \sigma\omega^{-1/2} \quad (3)$$

where ω is frequency, R_D is the charge transfer resistance, R_L is the electrolyte resistance. Based on the fitting linear equations in inset of Fig. 8, Li^+ diffusion coefficients of $NH_4V_3O_8$ and $NH_4V_3O_8$/0.5 wt% CNTs are about 2.92×10^{-13} cm^2 S^{-1} and 1.83×10^{-12} cm^2 S^{-1}, respectively. Apparently, addition of CNTs into bulk $NH_4V_3O_8$ is highly beneficial to Li^+ diffusion.

4. Conclusions

In summary, $NH_4V_3O_8$ composites with different contents of CNTs were prepared. Increasing the amount of CNTs could greatly improve discharge capacity. However, it also would form more $(NH_4)_{0.5}V_2O_5$ phase, leading to poorer structural stability. $NH_4V_3O_8$/0.5 wt% CNTs showed the best electrochemical performance with the maximum discharge capacity of 358.7 mAh g^{-1} at 30 mA g^{-1} and capacity retention of 97% after 100 cycles at 150 mA g^{-1}. The improved electrochemical performance was attributed to incorporation of CNTs, which facilitated the interface charge transfer and Li^+ diffusion. $NH_4V_3O_8$/0.5 wt% CNTs composite in this work indicates high discharge capacity and excellent cycling stability, which could be comparable to LiV_3O_8 with the best electrochemical performance to date. This work will open up a new direction to use $NH_4V_3O_8$, instead of LiV_3O_8 as cathode material for Li-ion battery.

Acknowledgements

Financial support from the Major State Basic Research Development Program of China (973 Program) (no. 2010CB227204), the National Natural Science Foundation of China (no. 50972165), Research Foundation of Hunan Province for Ph.D Student (no. CX2010B114), Graduate Degree Thesis Innovation Foundation of Central South University is greatly appreciated. H. Wang thanks to financial support from the Chinese government scholarship.

References

[1] M.S. Whittingham, Chem. Rev. 104 (2004) 4271–4302.
[2] J. Livage, Materials 3 (2010) 4175–4195.
[3] N.A. Chernova, M. Roppolo, A.C. Dillon, M.S. Whittingham, J. Mater. Chem. 19 (2009) 2526–2552.
[4] A.D. Wadsley, Acta Cryst. 10 (1957) 261–267.
[5] S. Panero, M. Pasquali, G. Pistoia, J. Electrochem. Soc. 130 (1983) 1225–1227.
[6] H.M. Liu, Y.G. Wang, K.X. Wang, Y.R. Wang, H.S. Zhou, J. Power Sources 192 (2009) 668–673.
[7] H.Y. Wang, K.L. Huang, S.Q. Liu, C.H. Huang, W.J. Wang, Y. Ren, J. Power Sources 196 (2011) 788–792.
[8] X.B. Huang, X. Li, H.Y. Wang, Z.L. Pan, M.Z. Qu, Z.L. Yu, Electrochim. Acta 55 (2010) 7362–7366.
[9] Z.W. Wang, M.D. Shirley, S.T. Meikle, R.L.D. Whitby, S.V. Mikhalovsky, Carbon 47 (2009) 73–79.
[10] C.C. Torardi, C.R. Miao, Chem. Mater. 14 (2002) 4430–4433.
[11] H.Y. Wang, K.L. Huang, C.H. Huang, S.Q. Liu, Y. Ren, X.B. Huang, J. Power Sources 196 (2011) 5645–5650.
[12] B. Azambre, M.J. Hudson, O. Heintz, J. Mater. Chem. 13 (2003) 385–393.
[13] A. Dobley, K. Ngala, S.F. Yang, P.Y. Zavalij, M.S. Whittingham, Chem. Mater. 13 (2001) 4382–4386.
[14] G. Pistoia, M. Pasquali, G. Wang, L. Li, J. Electrochem. Soc. 137 (1990) 2365–2370.
[15] Y.J. Kang, J.H. Kim, S.W. Lee, Y.K. Sun, Electrochim. Acta 50 (2005) 4784–4791.
[16] F. Nobili, F. Croce, B. Scrosati, R. Marassi, Chem. Mater. 13 (2001) 1642–1646.
[17] H.Y. Wang, K.L. Huang, S.Q. Liu, Y. Luo, Chin. J. Inorg. Chem. 25 (2009) 2090–2096.
[18] A.J. Bard, L.R. Faulkner, Electrochemical Methods, second ed., Wiley, 2001, p. 231.
[19] A.Y. Shenouda, H.K. Liu, J. Power Sources 185 (2008) 1386–1391.